C．研究結果

今年度は、イメージングプローブを構築するための準備段階という位置づけで研究を行った。上記ような研究方法により得られた結果から、

1．「ＰＴＤの設計とモデルタンパク質の構築」では、リジンとトリプトファンを組み合わせた新規ＰＴＤ配列を持ったＰＴＤ３融合タンパク質を構築することができた。

2．「培養細胞を用いたＰＴＤ融合タンパク質の細胞内輸送の検証」では、構築したＰＴＤ３融合タンパク質が効率に細胞内にＰＴＤ融合タンパク質を導入でき、融合したタンパク質の機能を発揮できることが分かった。

3．「動物実験での脳内輸送の検討」では、構築したＰＴＤ３融合タンパク質をネズミの腹腔内に投与することで、血液脳関門を通過し、効率よくデリバリーされることがわかった。

4．我々のグループで実際に検証して得られた上記のＰＴＤの情報を基に、ＰＴＤ３を用いたイメージングプローブ用融合たんぱく質の試作を行った。この試作した融合たんぱく質を用いて、次年度の研究を進める予定である。

D．考察

新規のＰＴＤ配列を用いたＰＴＤ融合タンパク質を全身投与で、脳にまで効率よく移行できた意義は大きいと考えられる。今後ＰＴＤを融合させたイメージングプローブのデリバリー効率を検討することにより、細胞内または生体内で任意の組織、および脳にまでイメージングプローブを効率よくデリバリーすることが出来るように工夫することができると考えられ、新規イメージングプローブを構築するために必要な準備がなされたと言える。

E．結語

本年度の結果を受けて、次年度以降に、マウスを使ってPTD-ODD融合たんぱく質の生体での動態を、まず免疫染色で、次にPTD-ODD融合たんぱく質を蛍光標識して、光イメージングで調べる。デリバリーや低酸素特異性を調べることで、問題点を検証し、PETプローブの開発に繋げたい。

G．研究発表

論文発表

1. S. Tachiiri, T. Katagiri, T. Tsunoda, N. Oya, M. Hiraoka and Y. Nakamura. Analysis of gene-expression profiles after gamma irradiation of normal human fibroblasts. Int J Radiat Oncol Biol Phys, 2006, 64:272-9.
2. T. Shibata, T. Shibata, Y. Maetani, H. Isoda and M. Hiraoka. Radiofrequency ablation for small hepatocellular carcinoma: prospective comparison of internally cooled electrode and expandable electrode. Radiology, 2006, 238:346-53.
3. N. Oya, K. Sasai, S. Tachiiri, T. Sakamoto, Y. Nagata, T. Okada, S. Yano, T. Ishikawa, T. Uchiyama and M. Hiraoka. Influence of radiation dose rate and lung dose on interstitial pneumonitis after fractionated total body irradiation: acute parotitis may predict interstitial pneumonitis. Int J

Hematol, 2006, 83:86-91.

4. T. Okada, Y. Miki, Y. Fushimi, T. Hanakawa, M. Kanagaki, A. Yamamoto, S. Urayama, H. Fukuyama, M. Hiraoka and K. Togashi. Diffusion-tensor fiber tractography: intraindividual comparison of 3.0-T and 1.5-T MR imaging. Radiology, 2006, 238:668-78.
5. H. Harada, S. Kizaka-Kondoh and M. Hiraoka. Antitumor protein therapy; application of the protein transduction domain to the development of a protein drug for cancer treatment. Breast Cancer, 2006, 13:16-26.
6. S. Zhu, T. Mizowaki, Y. Nagata, K. Takayama, Y. Norihisa, S. Yano and M. Hiraoka. Comparison of three radiotherapy treatment planning protocols of definitive external-beam radiation for localized prostate cancer. Int J Clin Oncol, 2005, 10:398-404.
7. Z. Zhang, H. Harada, K. Tanabe, H. Hatta, M. Hiraoka and S. Nishimoto. Aminopeptidase N/CD13 targeting fluorescent probes: synthesis and application to tumor cell imaging. Peptides, 2005, 26:2182-7.
8. C. Yamauchi, M. Mitsumori, Y. Nagata, M. Kokubo, T. Inamoto, K. Mise, H. Kodama and M. Hiraoka. Bilateral breast-conserving therapy for bilateral breast cancer: results and consideration of radiation technique. Breast Cancer, 2005, 12:135-9.
9. K. Takayama, Y. Nagata, Y. Negoro, T. Mizowaki, T. Sakamoto, M. Sakamoto, T. Aoki, S. Yano, S. Koga and M. Hiraoka. Treatment planning of stereotactic radiotherapy for solitary lung tumor. Int J Radiat Oncol Biol Phys, 2005, 61:1565-71.
10. M. Sakamoto, N. Oya, T. Mizowaki, N. Araki, Y. Nagata, K. Takayama, J. A. Takahashi, H. Kano, T. Katsuki, N. Hashimioto and M. Hiraoka. Initial Experiences of Palliative Stereotactic Radiosurgery for Recurrent Brain Lymphomas. J Neurooncol, 2005,
11. H. Sai, M. Mitsumori, N. Araki, T. Mizowaki, Y. Nagata, Y. Nishimura and M. Hiraoka. Long-term results of definitive radiotherapy for stage I esophageal cancer. Int J Radiat Oncol Biol Phys, 2005, 62:1339-44.
12. N. Oya, K. Shibuya, T. Sakamoto, T. Mizowaki, R. Doi, K. Fujimoto, M. Imamura, Y. Nagata and M. Hiraoka. Chemoradiotherapy in Patients with Pancreatic Carcinoma: Phase-I Study with a Fixed Radiation Dose and Escalating Doses of Weekly Gemcitabine. Pancreatology, 2005, 6:109-116.
13. M. Ogura, T. Shibata, J. Yi, J. Liu, R. Qu, H. Harada and M. Hiraoka. A tumor-specific gene therapy strategy targeting dysregulation of the VHL/HIF pathway in renal cell carcinomas. Cancer Sci, 2005, 96:288-94.
14. T. Nakayama, T. Tsuboyama, J. Toguchida, C. Tanaka, N. Oya, M. Hiraoka and T. Nakamura. Recurrence of osteosarcoma after intraoperative radiation therapy.

Orthopedics, 2005, 28:1195-7.

15. Y. Nagata, K. Takayama, Y. Matsuo, Y. Norihisa, T. Mizowaki, T. Sakamoto, M. Sakamoto, M. Mitsumori, K. Shibuya, N. Araki, S. Yano and M. Hiraoka. Clinical outcomes of a phase I/II study of 48 Gy of stereotactic body radiotherapy in 4 fractions for primary lung cancer using a stereotactic body frame. Int J Radiat Oncol Biol Phys, 2005, 63:1427-31.
16. M. Mitsumori, M. Hiraoka, Y. Negoro, C. Yamauchi, N. Shikama, S. Sasaki, T. Yamamoto, T. Teshima and T. Inoue. The patterns of care study for breast-conserving therapy in Japan: analysis of process survey from 1995 to 1997. Int J Radiat Oncol Biol Phys, 2005, 62:1048-54.
17. Lyshchik, T. Higashi, R. Asato, S. Tanaka, J. Ito, J. J. Mai, C. Pellot-Barakat, M. F. Insana, A. B. Brill, T. Saga, M. Hiraoka and K. Togashi. Thyroid gland tumor diagnosis at US elastography. Radiology, 2005, 237:202-11.
18. Lyshchik, T. Higashi, R. Asato, S. Tanaka, J. Ito, M. Hiraoka, A. B. Brill, T. Saga and K. Togashi. Elastic moduli of thyroid tissues under compression. Ultrason Imaging, 2005, 27:101-10.
19. J. Liu, R. Qu, M. Ogura, T. Shibata, H. Harada and M. Hiraoka. Real-time imaging of hypoxia-inducible factor-1 activity in tumor xenografts. J Radiat Res (Tokyo), 2005, 46:93-102.
20. H. Harada, S. Kizaka-Kondoh and M. Hiraoka. Optical imaging of tumor hypoxia and evaluation of efficacy of a hypoxia-targeting drug in living animals. Mol Imaging, 2005, 4:182-93.
21. Oka S, Masutani H, Liu W, Horita H, Wang D, Kizaka-Kondoh S, Yodoi J. Thioredoxin-binding protein-2 (TBP-2)-like inducible membrane protein (TLIMP) is a novel Vitamin D3- and PPAR-γ ligand target protein that regulates PPAR-γ signal. *Endocrinology*. 147(2):733-743 (2006).
22. Y Kageyama, H Sugiyama, H Ayame, A Iwai, Y Fujii, L Eric Huang, Kizaka-Kondoh S, Hiraoka M. and. Kihara K. Suppression of VEGF transcription in renal cell carcinoma cells using pyrrole-imidazole hairpin polyamides targeting the hypoxia responsive element. *Acta Oncologica*. In press.
23. 近藤科江、原田浩、平岡真寛。革新的診断・治療へのアプローチ；膜透過性・標的特異性を有する融合タンパク質を用いたイメージング、ターゲティング。BioClinica 20(1), 53-58. 2005
24. 近藤科江、平岡真寛、原田浩。がん治療における HIF-1 と Tumor Hypoxia. Cancer Frontier 7: 77-86 (2005).
25. 近藤科江。 Meeting Report がん分子標的治療研究会総会 がん分子標的治療 4(1), 62-64. 2006.
26. 近藤科江、原田浩、平岡真寛。『低酸素がん細胞』を標的としたがんのイメージング・ターゲティング バイオテクノロジージャーナル 6 (2), 234-237. 2006.

27. 近藤科江、原田浩、平岡真寛。低酸素を標的とした生体イメージング分子プローブの開発。未来医学。印刷中

学会発表

S. Kizaka-Kondoh, H. Harada, X. Xie, S. Itasaka, K. Shibuya, M. Hiraoka. Optical Imaging of HIF-1 activity in malignant solid tumors for evaluation of cancer therapies, Molecular Imaging, 4(3), 324, 2005. (Forth Annual Meeting, Cologne, Germany, September 7-10, 2005)

H．知的財産権の出願・登録状況

国際出願番号：PCT/JP2006/304701

発明の名称：病態の状態をリアルタイムで観察可能なモデル動物とそれを可能にする遺伝子構築物及びその使用

1) 発明者：近藤科江、原田浩、平岡真寛、山田秀一
2) 出願日：2006年3月10日
3) 出願人：**京都大学、関西ＴＬＯ**

厚生労働科学研究費補助金（萌芽的先端医療技術推進研究事業）
分担研究報告書

PETイメージングに関する研究

分担研究者　福山秀直　京都大学医学研究科　教授

研究要旨　MRIによって脳腫瘍切除時にどのような神経線維の走行や神経組織の圧迫による偏位が生じているかを、拡散強調画像を用いて評価し、その有用性について検討した。まず、従来の1.5テスラMRIと新しい強磁場3テスラMRIによる比較検討から、3テスラMRIが神経線維の描出にはるかに優れていることを明らかにした。続いて、脳動静脈奇形摘出術術中に電気刺激を用いて得られた視覚線維の走行部位と術前のMRIから推定された神経走行がほぼ一致することを示した。以上の結果から、MRI特に強磁場MRIによる神経線維走行の推定がより安全な脳腫瘍摘出を可能とすることが示唆された。

A. 研究目的

脳腫瘍の外科治療において、再発防止のためには十分に広範な摘出が必要である。一方、周囲の正常組織の機能を温存するためには、切除範囲を出来る限り小さくすることが望ましい。この治療範囲決定には、腫瘍周囲組織の機能を評価することが重要である。本研究では、MRIの拡散強調画像によるtractographyによって、腫瘍周囲の神経線維の種類と走行を評価し、その有用性を検討することを目的とした。

B. 研究方法

拡散強調画像を12方向撮像し、そのデータから拡散テンソル画像を求め、そのテンソルをボクセル毎に追跡し、必要な部位間の繊維連絡の有無を検討した。使用したソフトウェアは主にDTI studioと呼ばれる米国ジョンズ・ホプキンス大学の森助教授が開発したプログラムである。3テスラMRIによって得られた画像と1.5テスラMRIによって得られた画像を比較検討した。さらに、脳動静脈奇形切除中の電気刺激を用いて得られた視覚線維の走行部位と術前のMRI画像から推定された神経走行部位の異動について検討を行った。

（倫理面への配慮）本研究は京都大学医学部倫理委員会の承認を得て、すべての被検者に口頭および文書にて十分な説明を行い文書による同意を得て行った。

C. 研究結果

3テスラMRIによって得られた画像は1.5テスラMRIによって得られた画像と比較して、S/Nに優れ、より詳細な検討を可能とした[1]。脳動静脈奇形摘出術中の電気刺激によって得られた視覚線維の走行部位と術前MRI画像から推定された神経走行部位では大きな差異のないことを確認した[2]。

D. 考察

物理的性質より予想された強磁場MRIのtractography画像における優位性を臨床の場で証明された。また、病変として安定している脳動静脈奇形摘出術術中に電気刺激を用いて得られた視覚線維の走行部位とMRI画像から推定された神経走行部位の一致は、脳腫瘍にも応用可能であり、切除範囲決定に有用な情報が得られることが予想された。

E. 結論

MRIによるtractographyによって、神経線維の種類および走行を確認することによって、より安全で適切な脳腫瘍摘出術が可能となることが示された。

F. 健康危険情報　なし。

G. 研究発表

1．論文発表

1) Okada T, Fukushima H, et al. Radiology 2006;238:668-678.
2) Kikuta K, Fukuyama H, et al. Neursurgery 2006;58:331-337.

H.　知的財産権の出願・登録状況　なし。

厚生労働化学研究費補助金（萌芽的先端医療技術推進研究事業）
分担研究報告書

PETイメージングに関する研究

分担研究者　　中本　裕士　　京都大学医学研究科放射線医学講座・助手

研究要旨：　原発性脳腫瘍の診断におけるFLT-PETの有用性を、FDG-PETと比較検討した。FLT-PETとFDG-PETでは、原発性脳腫瘍の悪性度診断能において大きな差異を認めなかったが、FLT-PETの方がコントラスト良く腫瘍を描出可能で、腫瘍内の集積の不均一性もより明瞭であった。適正な生検部位の決定や治療計画の応用には、FLT-PETの方が適していると考えられた。

A．研究目的

フッ素-18標識フルオロチミジンを用いたポジトロン断層法（FLT-PET）は、腫瘍の増殖能を非侵襲的に評価可能と期待されている。原発性脳腫瘍の診断におけるFLT-PETの有用性を、FDG-PETと比較検討する。

B．研究方法

原発性脳腫瘍の疑われた患者8名にFLT-PETおよびFDG-PET検査を施行した。FLTないしFLT約370MBqを静脈内投与し、40分後からエミッションスキャン20分、トランスミッションスキャン3分のデータ収集を行った。再構成された画像上に、関心領域を設定し、FLTおよびFDGの腫瘍への集積(SUV: standardized uptake valueおよびTNR: tumor-to-normal brain ratio)を測定し、組織学的に決定された腫瘍の悪性度、増殖能と対比した。

（倫理面への配慮）

FLT-PETの研究内容は、医学研究科・医の倫理委員会の承認を得た。被検者に研究内容を文書にて説明し、同意を得て、検査を施行した。

C．研究結果

FDGは正常脳に高い集積を認めるのに対し、FLTは正常脳への集積をほとんど認めなかった。8名の組織診断は、grade2の神経膠腫が3例、grade3の神経膠腫が2例、悪性度の高い神経膠芽腫が2例、悪性リンパ腫が1例であった。腫瘍のSUV値は、悪性リンパ腫の1例を除いて、FDGの方がFLTよりも高い値を呈したのに対し、TNRは全例でFLTの方が高値で、FLT-PETにおいて腫瘍が高コントラストに描出され、腫瘍内の集積の不均一性もFLT-PETで評価が容易であった。組織学的悪性度との比較では、ともに1例の偽陽性例を認めたが、それ以外では、FLT、FDGともにその集積性が悪性度を反映する傾向が見られた。また、FLTのSUV値、TNR値とFDGのSUV値、TNR値はそれぞれ相関する傾向が見られた。

D．考察

理論的には、細胞増殖のマーカーであるFLTの方が、腫瘍の悪性度をよりよく反映す

ると期待されたが、今回の検討では、FLTとFDGの間に大きな差を認めなかった。症例が少ないこともあるが、細胞増殖に加え、糖代謝亢進も悪性度と強く関連していることによると考えられる。しかし、正常脳への集積の非常に低いFLTの方が、腫瘍の描出が良好で、腫瘍内の集積の評価も容易であった。この点で、FLT-PETの方が、腫瘍内の高悪性度部位の検出に優れると思われ、適正な生検部位の決定、放射線治療計画への応用(dose painting)にはより適していると考えられる。

E．結論

症例数が限られているが、FLT、FDGともに、原発性脳腫瘍の組織学的悪性度を反映して集積する傾向が見られた。しかし、腫瘍と正常脳組織のコントラストは、FLT-PETの方が優れており、腫瘍組織内での不均一性の検出、適正な生検部位の決定や治療計画への応用には、FLTの方が適していると考えられた。

F．健康危険情報

FLT-PET、FDG-PET検査に起因すると思われる副作用を経験していない。

G．研究発表

1．論文発表

なし

2．学会発表

（発表誌名巻号・頁・発行年等も記入）

第45回日本核医学会総会(平成17年11月12日、東京)

第91回北米放射線学会(平成17年12月、シカゴ)

第65回日本医学放射線学会総会・学術集会(平成18年4月7-9日、横浜)にて発表予定

H．知的財産権の出願・登録状況

（予定を含む）

1．特許取得

なし

2．実用新案登録

なし

3．その他

なし

厚生労働科学研究助成金（萌芽的先端医療技術推進研究事業）
分担研究報告書

PETイメージングに関する研究・近接撮像型フレキシブル分子イメージング装置の開発

分担研究者　村山　秀雄　放射線医学総合研究所研究員

研究要旨

放医研における次世代 PET 装置開発プロジェクトで開発された４層-DOI 検出器は、GSO シンチレータのみに提供できる技術であったが、光分配方式のみによる４層 DOI 方式が成功し、一種類のシンチレータ素子で４層 DOI 検出器が構成できるようになった。また、２つの受光素子に跨るシンチレータについて基礎研究を行い、２層 DOI が可能であることを示した。８層 DOI 方式が可能であることを実験室段階で実証した。

A．研究目的

高感度かつ高解像度を達成するための PET 装置用ｹ検出器を研究開発すると共に、分子イメージング画像の定量性 を向上する測定法を研究開発する。

B．研究方法

256ch FP-PMT の上に、1.45mm×1.45mm×4.5mm の LSO シンチレータを 32x8x4 層に配置する３次元小型結晶配列は、次世代 PET 開発研究の中で放医研が開発した技術を下に新たな光学的制御を工夫して試作を行った。4 層 DOI 検出器に対する応答関数実験を体軸方向、深さ方向それぞれに行った。さらに、22Na 線源から鉛こりメータで直径 1 mm の消滅放射線ビームを出し、0.5 mm ピッチでスキャンしながら 4 層 DOI 検出器に照射した。

C．研究結果

検出器ユニットを２つ作成し、同時計数測定を行った結果、1.5 mm の空間分解能を得た。以上の結果から、4 層 LSO-DOI 検出器の開発により、検出器リング径が 8cm と小さく、体軸方向に長い超高感度の小動物用 PET 装置をシステムデザインした。また、DOI 検出器を PET 装置用として実用化する際に、受光素子間の隙間を検出素子で埋めて、感度とサンプリングの低下を防ぐ方法を検討した。さらに、８層 DOI 検出器が実現可能であることを、GSO を用いた３次元結晶配列ブロックと 256ch FP-PMT を用いて試作し実験室の段階で実証した。

D．考察

本研究で開発された４層-DOI 方式は、シンチレータの種類に依らない。また、波形弁別方式を利する必要がなくなったので、小型・高速性を要求される少動物用 PET 装置の検出器として適している。８層 DOI 方式は近接撮像型フレキシブル分子イメージングに活用が期待できる。

E．考察

光分配方式のみによる４層 DOI 方式が成功し、一種類のシンチレータ素子で４層 DOI 検出器が構成できるようになった。また、２つの受光素子に跨るシンチレータについて基礎研究を行い、２層 DOI が可能であることを示した。８層 DOI 方式が可能であることを実験室段階で実証した。

G．研究発表

１．論文発表

1. Hasegawa, T., Ishikawa, M., Maruyama, K., Inadama, N., Yoshida, E., Murayama, H. : Depth-of-interaction recognition using optical filters for nuclear medicine imaging. IEEE Trans. Nucl. Sci., 52(1), pp. 4-7, 2005.

2. Orita, N., Murayama, H., Kawai, H., Inadama, N., Tsuda, T. : Three-dimensional array of scintillation crystals with proper reflector arrangement for a depth of interaction detector. IEEE Trans. Nucl. Sci., 52(1), pp. 8-14, 2005.

3. Inadama, N., Murayama, H., Watanabe, M., Omura, T. , Yamashita, T., Kawai, H., Orita, N., Tsuda, T. : Performance of a 256ch Flat Panel PS-PMT with small crystals for a DOI PET detector. IEEE Trans. Nucl. Sci., 52(1), pp. 15-20, 2005.

4. Yamamoto, S., Takamatsu, S., Murayama, H., Minato, K. : A block detector for a multislice, depth-of-interaction MR-compatible PET. IEEE Trans. Nucl. Sci., 52(1), pp. 33-37, 2005.

5. 山谷泰賀, 北村圭司, 萩原直樹, 小尾高史, 長谷川智之, 吉田英治, 津田倫明, 稲玉直子, 和田弘康, 村山秀雄 : 小動物用 DOI-PET 装置 "jPET-RD" の 2 次元イメージングシミュレーション. 医学物理, 25(1), pp.13-23, 2005.

6. 山谷泰賀, 吉田英治, 佐藤允信, 津田倫明, 北村圭司, 萩原直樹, 小尾高史, 長谷川智之, 羽石秀昭, 稲玉直子, 澁谷憲悟, 森慎一郎, 遠藤真広, 棚田修二, 村山秀雄 : DOIC 法を用いた 1 リング jPET-D4 試作機のイメージング性能評価. Med. Imag. Tech., 23(4), pp.185-193, 2005.

7. Yamaya, T., Hagiwara, N., Obi, T., Yamaguchi, M., Ohyama, N., Kitamura, K., Hasegawa, T., Haneishi, H., Yoshida1, E., Naoko Inadama, N., Murayama, H. : Transaxial system models for jPET-D4 image reconstruction. Phys. Med. Biol., 50, pp. 5339-5355, 2005.

2．学会発表

1. Yamaya, T., Yoshida, E., Satoh, M., Tsuda, T., Kitamura, K., Obi, T., Hasegawa, T., Haneishi, H., Inadama, N., Tanada, S., Murayama, H. : The jPET-D4: Transaxial imaging performance of a novel 4-layer depth-of-interaction. Proc. part 1 of the 4th Japan-Korea Joint Meeeting on Medical Physics and the 5th Asia-Oceania Congress of Medical Physics, Kyoto, Sept. 28 - Oct. 1, Jpn. J. Med. Phys., 25, Sup.3-1, pp.111-114, 2005.

2. Ono, Y., Murayama, H., Yamaya, T., Kawai, H., Imadama, N., Tsuda, T., Hamamoto, M. : Four-layer depth-of-interaction detectors for the jPET-D4. Proc. part 1 of the 4th Japan-Korea Joint Meeeting on Medical Physics and the 5th Asia-Oceania Congress of Medical Physics, Kyoto, Sept. 28 -Oct. 1, Jpn. J. Med. Phys., 25, Sup.3-1, pp.115-118, 2005.

3. Inadama, N., Murayama, H., Yamaya, T., Tsuda, T., Ono, Y., Hamamoto, M. : DOI detection capability of 3D crystal array standing over two PMTs. Proc. part 1 of the 4th Japan-Korea Joint Meeeting on Medical Physics and the 5th Asia-Oceania Congress of Medical Physics, Kyoto, Sept. 28 -Oct. 1, Jpn. J. Med. Phys., 25, Sup.3-1, pp.119-122, 2005.

4. Hamamoto, M., Murayama, H., Inadama, N., Tsuda, T., Ono, Y., Yamaya, T., Yoshida, E., Shibuya, K., Nishikido, F., Kikuchi, J., Doke, T. : 8-layer depth-of-interaction encoding of 3-dimensional crystal array. Proc. part 1 of the 4th Japan-Korea Joint Meeeting on Medical Physics and the 5th Asia-Oceania Congress of Medical Physics, Kyoto, Sept. 28 -Oct. 1, Jpn. J. Med. Phys., 25, Sup.3-1, pp.123-126, 2005.

5. Tsuda, T., Murayama, H., Kitamura, K., Imadama, N., Yamaya, T., Yoshida, E., Nishikido, F., Hamamoto, M., Kawai, H., Ono, Y. : Resolution measurements of a four-layer DOI prototype detector for jPET-RD. Proc. part 2 of the 4th Japan-Korea Joint Meeeting on Medical Physics and the 5th Asia-Oceania Congress of Medical Physics, Kyoto, Sept. 28 - Oct. 1, Jpn. J. Med. Phys., 25, Sup.3-2, pp.32-34, 2005.

6. Yoshida, E., Satoh, M., Kitamura, K., Yamaya, T., Murayama, H. : Calibration and evaluation of DOI detector for jPET-D4. Proc. part 2 of the 4th Japan-Korea Joint Meeeting on Medical Physics and the 5th Asia-Oceania Congress of Medical Physics, Kyoto, Sept. 28 -Oct. 1, Jpn. J. Med. Phys., 25, Sup.3-2, pp.42-44, 2005.

7. Fukushima, Y., Hasegawa, T., Muraishi, H., Nakano, T., Kuribayashi, T., Shiba, Y., Maruyama, K., Yamaya, T., Yoshida, E., Hagiwara, N., Obi, T., Murayama, H. : Accuracy measurement with a high-precision solid marker for PET head motion correction. Proc. part 2 of the 4th Japan-Korea Joint Meeeting on Medical Physics and the 5th Asia-Oceania Congress of Medical Physics, Kyoto, Sept. 28 - Oct. 1, Jpn. J. Med. Phys., 25, Sup.3-2, pp.52-54, 2005.

8. Shibuya, K., Inadama, N., Yoshida, E., Yamaya, T., Murayama, H., Saito, H., Koshimizu, M., Asai, K. : Low-dimensional semiconducting materials in developing ultra-fast scintillators. Proc. part 2 of the 4th Japan-Korea Joint Meeeting on Medical Physics and the 5th Asia-Oceania Congress of Medical Physics, Kyoto, Sept. 28 -Oct. 1, Jpn. J. Med. Phys., 25, Sup.3-2, pp.179-182, 2005.

9. Ogane, K., Ishikawa, M., Hirasawa, M., Tomitani, T., Murayama, H., Takahashi, H., Nakazawa, M. : Feasibility study on a noninvasive measurement system for boron concentration. Proc. part 2 of the 4th Japan-Korea Joint Meeeting on Medical Physics and the 5th Asia-Oceania Congress of Medical Physics, Kyoto, Sept. 28 -Oct. 1, Jpn. J. Med. Phys., 25, Sup.3-2, pp.208-210, 2005.

10. Hasegawa, T., Fukushima, Y., Isobe, T., Umezawa, N., Maruyama, K., Umeda, T., Muraishi, H., Murayama, H., Yaguchi, Y., Kojima, H., Miwa, K. : 3D animations for medical physics education and learning. Proc. part 2 of the 4th Japan-Korea Joint Meeeting on Medical Physics and the 5th Asia-Oceania Congress of Medical Physics, Kyoto, Sept. 28 - Oct. 1, Jpn. J. Med. Phys., 25, Sup.3-2, pp.260-263, 2005.

11. Yeom, J.Y., Defendi, I., Takahashi, H.,

Zeitelhack, K., Nakazawa, M., Murayama, H. : A 12-channel CMOS preamplifier-shaper-discriminator ASIC for APD and gas counters. 2005 IEEE Nuc. Sci. Sympo. & Med. Imag. Conf. Record., N14-34, 2005.

12. Shibuya, K., Inadama, N., Yoshida, E., Yamaya, T., Murayama, H., Koshimizu, M., Asai, K. : Quantum confinement effects in semiconducting scintillators. 2005 IEEE Nuc. Sci. Sympo. & Med. Imag. Conf. Record., N38-2, 2005.

13. Inadama, N., Murayama, H., Hamamoto, M., Tsuda, T., Ono, Y., Yamaya, T., Yoshida, E., Shibuya, K., Nishikido, F., Kikuchi, J., Doke, T. : 8-layer depth-of-interaction encoding of 3-dimensional crystal array. 2005 IEEE Nuc. Sci. Sympo. & Med. Imag. Conf. Record., N38-2, 2005.

14. Tsuda, T., Murayama, H., Kitamura, K., Imadama, N., Yamaya, T., Yoshida, E., Nishikido, F., Hamamoto, M., Kawai, H., Ono, Y. : Measurement of 32x8x4 LYSO crystal responses of DOI detector for jPET-RD. 2005 IEEE Nuc. Sci. Sympo. & Med. Imag. Conf. Record., J3-28, 2005.

15. Hamamoto, M., Inadama, N., Murayama, H., Yamaya, T., Tsuda, T., Ono, Y. : DOI detection capability of 3D crystal array standing over two PMTs. 2005 IEEE Nuc. Sci. Sympo. & Med. Imag. Conf. Record., M3-115, 2005.

16. Hasegawa, T., Fukushima, Y., Muraishi, H., Nakano, T., Kuribayashi, T., Shiba, Y., Maruyama, K., Yamaya, T., Yoshida, E., Murayama, H., Hagiwara, N., Obi, T. : Motion correction for jPET-D4: improvement of measurement accuracy with a solid marker. 2005 IEEE Nuc. Sci. Sympo. & Med. Imag. Conf. Record., M3-244, 2005.

17. Yoshida, E., Kimura, Y., Kitamura, K., Nishikido, F., Yamaya, T., Murayama, H. : Event-by-event random and scatter estimator based on support vector machine using multi-anode outputs. 2005 IEEE Nuc. Sci. Sympo. & Med. Imag. Conf. Record., M3-304, 2005.

18. Yamaya, T., Yoshida, E., Satoh, M., Tsuda, T., Kitamura, K., Obi, T., Hasegawa, T., Haneishi, H., Inadama, N., Tanada, S., Murayama, H. : The jPET-D4: imaging performance of the 4-layer depth-of-interaction PET scanner. 2005 IEEE Nuc. Sci. Sympo. & Med. Imag. Conf. Record., M7-83, 2005.

19. Ono, Y., Murayama, H., Yamaya, T., Kawai, H., Imadama, N., Tsuda, T., Hamamoto, M. : The jPET-D4: simple and reliable construction method for 4-layer DOI crystal blocks. 2005 IEEE Nuc. Sci. Sympo. & Med. Imag. Conf. Record., M11-111, 2005.

20. Yoshida, E., Yamaya, T., Watanabe, M., Inadama, N., Tsuda, T., Kitamura, K., Hasegawa, T., Obi, T., Haneishi, H., Murayama, H. : The jPET-D4: calibration and acquisition system of the 4-layer DOI-PET scanner. 2005 IEEE Nuc. Sci. Sympo. & Med. Imag. Conf. Record., M11-270, 2005.

H. 知的財産の出願・登録状況

1. 特許出願

1. 稲玉直子, 村山秀雄, 澁谷憲悟, 北村圭司, 石橋浩之：放射線位置検出方法及び装置, 平成 17 年 9 月 28 日出願、出願番号　特願 2005-282866

2. 北村圭司, 吉田英治, 村山秀雄, 木村裕一：放射線同時計数処理方法、放射線同時計数処理プログラム、および放射線同時計数処理記憶媒体並びに放射線同時計数装置およびそれを用いた核医学診断装置, 平成 17 年 10 月 20 日出願、出願番号　特願 2005-305944

2. 特許登録

1.村山秀雄, 石橋浩之, 山下貴司, 内田博, 大村知秀：放射線入射位置 3 次元検出器の発行位置特定方法, 平成 17 年 7 月 8 日登録、特許第 3697340 号

研究成果の刊行に関する一覧表

書籍

著者氏名	論文タイトル名	書籍全体の編集者名	書　籍　名	出版社名	出版地	出版年	ページ
なし							

雑誌

発表者氏名	論文タイトル名	発表誌名	巻号	ページ	出版年
Kuge Y, Katada Y, Shimonaka S, Temma T, Kimura H, Kiyono Y, Yokota C, Minematsu K, Seki K, Tamaki N, Ohkura K, Saji H.	Synthesis and evaluationof radioiodinated cyclooxygenase-2 inhibitors as potential SPECT tracers for cyclooxygenase-2 expression.	Nucl Med Biol	33(1)	21-27	2006
Ogawa K, Mukai T, Arano Y, Ono M, Hanaoka H, Ishino S, Hashimoto K, Nishimura H, Saji H.	Development of a rhenium-186-labeled MAG3-conjugated bisphosphonate for the palliation of metastatic bone pain based on the concept of bifunctional radiopharmaceuticals.	Bioconjugate Chem.	16(4)	751-757	2005
Obata A, Kasamatsu S, Lewis JS, Furukawa T, Takamatsu S, Toyohara J, Asai T, Welch MJ, Adams SG, Saji H, Yonekura Y, Fujibayashi Y.	Basic characterization of ^{64}Cu-ATSM as a radiotherapy agent.	Nucl Med Biol	32(1)	21-28	2005
Hanaoka H, Mukai T, Tamamura H, Mori T, Ishino S, Ogawa K, Iida Y, Doi R, Fujii N, Saji H.	Development of a ^{111}In-labeled peptide derivative targeting a chemokine receptor, CXCR4, for imaging tumors.	Nucl Med Biol	In press		

Takei T, Kuge Y, Zhao S, 他	Enhanced apoptotic reaction correlates with suppressed tumor glucose utilization after cytotoxic chemotherapy: use of ^{99m}Tc-Annexin V, ^{18}F-FDG, and histologic evaluation.	J Nucl Med.	46(5)	794-799	2005
Zhao S, Kuge Y, Mochizuki T, 他	Biologic correlates of intratumoral heterogeneity in 18F-FDG distribution with regional expression of glucose transporters and hexokinase-II in experimental tumor.	J Nucl Med.	46(4)	675-682	2005
J. Liu, R. Qu, M. Ogura, T. Shibata, H. Harada and M. Hiraoka.	Real-time imaging of hypoxia-inducible factor-1 activity in tumor xenografts	J Radiat Res (Tokyo)	46	93-102	2005
H. Harada, S. Kizaka-Kondoh and M. Hiraoka	Optical imaging of tumor hypoxia and evaluation of efficacy of a hypoxia-targeting drug in living animals.	Mol Imaging	4	182-93	2005
M. Ogura, T. Shibata, J. Yi, J. Liu, R. Qu, H. Harada and M. Hiraoka	A tumor-specific gene therapy strategy targeting dysregulation of the VHL/HIF pathway in renal cell carcinomas	Cancer Sci	96	288-94	2005
H. Harada, S. Kizaka-Kondoh and M. Hiraoka.	Antitumor protein therapy; application of the protein transduction domain to the development of a protein drug for cancer treatment.	Breast Cancer	13	16-26	2006
Y Kageyama, H Sugiyama, H Ayame, A Iwai, Y Fujii, L Eric Huang, Kizaka-Kondoh S, Hiraoka M. and. Kihara K.	Suppression of VEGF transcription in renal cell carcinoma cells using pyrrole-imidazole hairpin polyamides targeting the hypoxia responsive element	*Acta Oncologica.*	In press		
近藤科江、原田浩、平岡真寛	革新的診断・治療へのアプローチ；膜透過性・標的特異性を有する融合タンパク質を用いたイメージング、ターゲティング	BioClinica	20(1)	53-58	2005
近藤科江、平岡真寛、原田浩	がん治療におけるHIF-1とTumor Hypoxia	Cancer Frontier	7	77-86	2005

近藤科江、原田浩、平岡真寛	『低酸素がん細胞』を標的としたがんのイメージング・ターゲティング	バイオテクノロジージャーナル	6 (2)	234-237	2006
近藤科江、原田浩、平岡真寛	低酸素を標的とした生体イメージング分子プローブの開発	未来医学	印刷中		
Okada T, Miki Y, Fushimi Y, Hanakawa T, Kanagaki M, Yamamoto A, Urayama S, Fukushima H, et al.	Diffusion-tensor fiber tractography: intra individual comparison of 3.0-T and 1.5T MR imaging.	Radiology	238	668-678	2006
Kikuta K, Takagi Y, Nozaki K, Hanakawa T, Okada T, Miki Y, Fushimi Y, Fukuyama H, Hashimoto N	Early experiment with 3-T magnetic resonance tractography in the surgery of cerebral arteriovenous malformations in and around the visual pathway.	Neurosurgery	58	331-337	2006

Available online at www.sciencedirect.com
SCIENCE DIRECT
Nuclear Medicine and Biology 33 (2006) 21–27
NUCLEAR MEDICINE — AND — BIOLOGY
www.elsevier.com/locate/nucmedbio

Synthesis and evaluation of radioiodinated cyclooxygenase-2 inhibitors as potential SPECT tracers for cyclooxygenase-2 expression

Yuji Kuge[a,*], Yumiko Katada[a], Sayaka Shimonaka[a], Takashi Temma[a], Hiroyuki Kimura[a], Yasushi Kiyono[b], Chiaki Yokota[c], Kazuo Minematsu[d], Koh-ichi Seki[e], Nagara Tamaki[f], Kazue Ohkura[g], Hideo Saji[a]

[a]*Department of Patho-Functional Bioanalysis, Graduate School of Pharmaceutical Sciences, Kyoto University, Kyoto 606-8501, Japan*
[b]*Radioisotopes Research Laboratory, Kyoto University Hospital, Faculty of Medicine, Kyoto University, Kyoto 606-8507, Japan*
[c]*Cerebrovascular Laboratory, National Cardiovascular Center Research Institute, Osaka 565-8565, Japan*
[d]*Cerebrovascular Division, Department of Medicine, National Cardiovascular Center Research Institute, Osaka 565-8565, Japan*
[e]*Central Institute of Isotope Science, Hokkaido University, Hokkaido 060-8638, Japan*
[f]*Department of Nuclear Medicine, Graduate School of Medicine, Hokkaido University, Hokkaido 060-8638, Japan*
[g]*Department of Radiopharmaceutical Chemistry, Faculty of Pharmaceutical Sciences, Health Sciences University of Hokkaido, Hokkaido 061-0293, Japan*

Received 26 August 2005; received in revised form 30 September 2005; accepted 5 October 2005

Abstract

Although several COX-2 inhibitors have recently been radiolabeled, their potential for imaging COX-2 expression remains unclear. In particular, the sulfonamide moiety of COX-2 inhibitors may cause slow blood clearance of the radiotracer, due to its affinity for carbonic anhydrase (CA) in erythrocytes. Thus, we designed a methyl sulfone-type analogue, 5-(4-iodophenyl)-1-[4-(methylsulfonyl)phenyl]-3-trifluoromethyl-1*H*-pyrazole (IMTP). In this study, the potential of radioiodinated IMTP was assessed in comparison with a ^{125}I-labeled celecoxib analogue with a sulfonamide moiety (^{125}I-IATP).

Methods: The COX inhibitory potency was assessed by measuring COX-catalyzed oxidation by hydrogen peroxide. The biodistribution of ^{125}I-IMTP and ^{125}I-IATP was determined by the ex vivo tissue counting method in rats. Distribution of the labeled compounds to rat blood cells was measured.

Results: The COX-2 inhibitory potency of IMTP (IC_{50}=5.16 μM) and IATP (IC_{50}=8.20 μM) was higher than that of meloxicam (IC_{50}=29.0 μM) and comparable to that of SC-58125 (IC_{50}=1.36 μM). The IC_{50} ratios (COX-1/COX-2) indicated the high isoform selectivity of IMTP and IATP for COX-2. Significant levels of ^{125}I-IMTP and ^{125}I-IATP were observed in the kidneys and the brain (organs known to express COX-2). The blood clearance of ^{125}I-IMTP was much faster than that of ^{125}I-IATP. Distribution of ^{125}I-IATP to blood cells (88.0%) was markedly higher than that of ^{125}I-IMTP (18.1%), which was decreased by CA inhibitors.

Conclusions: Our results showed a high inhibitory potency and selectivity of IMTP for COX-2. The substitution of a sulfonamide moiety to a methyl sulfone moiety effectively improved the blood clearance of the compound, indicating the loss of the cross reactivity with CA in ^{125}I-IMTP. ^{123}I-IMTP may be a potential SPECT radiopharmaceutical for COX-2 expression.

Keywords: Cyclooxygenase-2 (COX-2); Inhibitor; Radioiodination; SPECT; Radiopharmaceutical

1. Introduction

Cyclooxygenases (COXs) catalyse the key rate-limiting step in the conversion of arachidonic acid into prostaglandins and thromboxanes. To date, at least 2 distinct isoforms of the COXs—a constitutive form (COX-1) and an inducible isoform (COX-2)—and several of their variants have been discovered [1]. COX-1 is constitutively expressed in most tissues and is responsible for maintaining homeostasis, whereas COX-2 is induced in response to inflammatory stimuli. Besides being associated with inflammation, COX-2 has been implicated in a number of pathological processes, including many human cancers, atherosclerosis, and cerebral and cardiac ischemia [2–5]. We also reported

* Corresponding author. Tel.: +81 75 753 4608; fax: +81 75 753 4568.
E-mail address: kuge@pharm.kyoto-u.ac.jp (Y. Kuge).

0969-8051/$ – see front matter © 2006 Elsevier Inc. All rights reserved.
doi:10.1016/j.nucmedbio.2005.10.004

the neuronal expression of COX-2 in rodent and primate models of cerebral ischemia [6–10].

Accordingly, the noninvasive imaging of COX-2 expression should help in understanding the pathophysiology of the diseases and contribute to the clinical use of COX-2 inhibitors [11]. In this regard, several COX-2 inhibitors were recently radiolabeled with F-18 and their potentials for positron emission tomography (PET) tracers were preliminarily evaluated [12–14]. The results for the potentials of these labeled compounds, however, are not necessarily consistent from one laboratory to another. In addition, the short half-life of ^{18}F may hamper the determination of the specific binding of the tracer to COX-2, because it is known that the COX-2 inhibitors show time-dependent inhibition of COX-2 [11]. The longer half-lives of single photon emission tomography (SPECT) nuclides, such as Tc-99m or I-123, may be more suitable for radiotracers to image COX-2. From these points of view, we intended to develop radioiodinated COX-2 inhibitors as SPECT tracers for imaging COX-2 expression.

As for SPECT tracers, Yang et al. [15] proposed a ^{99m}Tc-labeled celecoxib (celebrex) analogue as a potential tracer for COX-2 expression. Kabalka et al. [16] recently reported the radiosynthesis of a ^{123}I-labeled celecoxib analogue. However, the detailed characteristics of these tracers, including affinity and selectivity to COX-2, have not

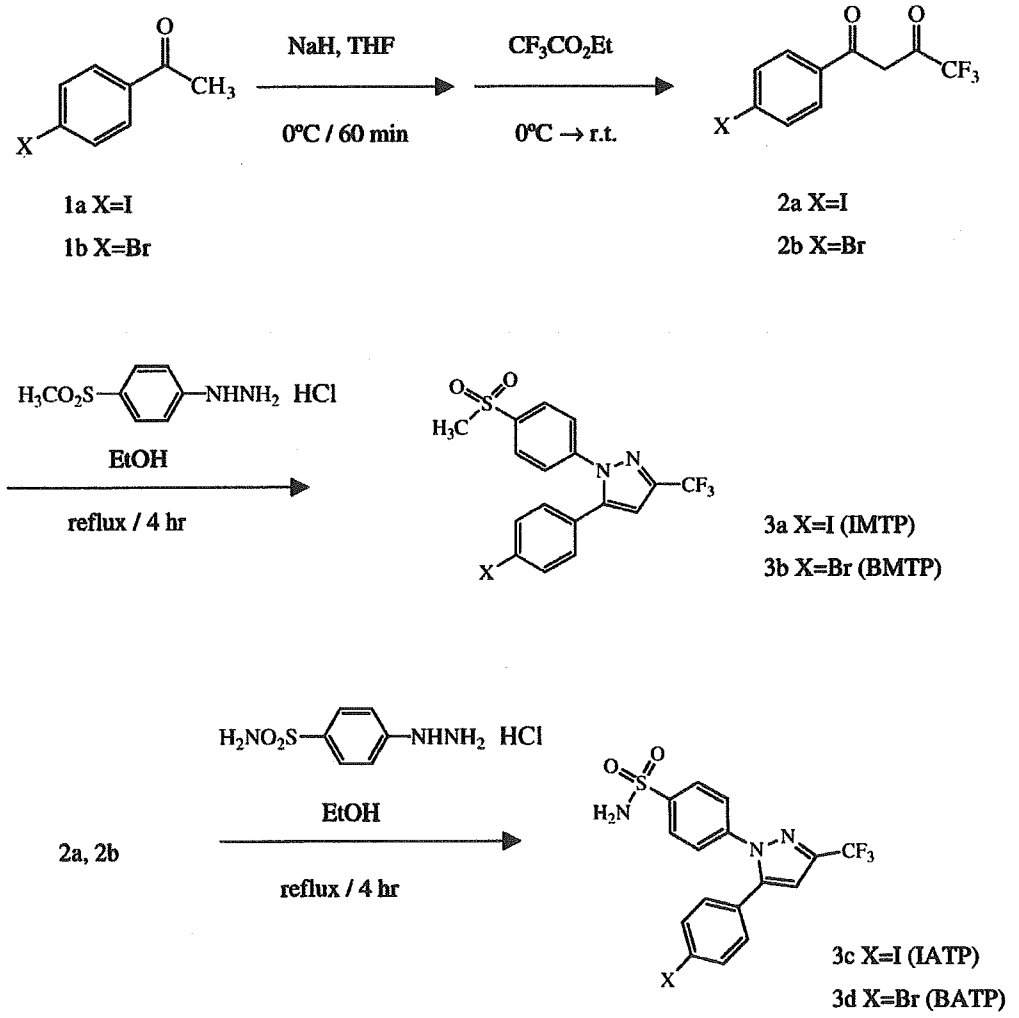

Fig. 1. Synthesis of IMTP (compound **3a**), BMTP (compound **3b**), IATP (compound **3c**) and BATP (compound **3d**).
Compound 1a, iodoacetophenone
Compound 1b, bromoacetophenone
Compound 2a, 4,4,4-trifluoro-1-(4-iodophenyl)-butane-1,3-dione
Compound 2b, 4,4,4-trifluoro-1-(4-bromophenyl)-butane-1,3-dione
Compound 3a, 5-(4-iodophenyl)-1-[4-(methylsulfonyl)phenyl]-3-trifluoromethyl-1H-pyrazole
Compound 3b, 5-(4-bromophenyl)-1-[4-(methylsulfonyl)phenyl]-3-trifluoromethyl-1H-pyrazole
Compound 3c, 5-(4-iodophenyl)-1-[4-(aminosulfonyl)phenyl]-3-trifluoromethyl-1H-pyrazole
Compound 3d, 5-(4-bromophenyl)-1-[4-(aminosulfonyl)phenyl]-3-trifluoromethyl-1H-pyrazole

been determined and their usefulness remains unclear. In particular, the sulfonamide moiety of celecoxib may cause slow blood clearance of the radiotracer, due to its affinity for carbonic anhydrase in erythrocytes [17,18].

Thus, we designed a methyl sulfone-type analogue, 5-(4-iodo-phenyl)-1-[4-(methylsulfonyl)phenyl]-3-trifluoromethyl-1*H*-pyrazole (IMTP), iodinated at position 4 of the 5-phenyl ring as a SPECT tracer for imaging COX-2 expression (Fig. 1). In this study, radioiodinated IMTP was synthesized, and its potential was assessed in comparison with a ^{125}I-labeled cerecoxib analogue with a sulfonamide moiety (^{125}I-IATP).

2. Materials and methods

2.1. General

Sodium ^{125}I-iodide (642.8 GBq/mg) was purchased from Perkin Elmer Life and Analytical Sciences (Boston, MA). All chemicals used were of reagent grade.

Proton nuclear magnetic resonance (^{1}H NMR) spectra were recorded on a JNM-EX 400 spectrometer (JEOL, Tokyo, Japan), and the chemical shifts were reported in parts per million (ppm) downfield from an internal tetramethylsilane standard. Fast atom bombardment (FAB) mass spectra were recorded with a JMS-HX/HX110A model spectrometer (JEOL).

2.2. Synthesis

2.2.1. 5-(4-Iodophenyl)-1-[4-(methylsulfonyl)phenyl]-3-trifluoromethyl-1H-pyrazole (IMTP)

IMTP was synthesized according to the procedure outlined in Fig. 1. To dry tetrahydrofuran (THF, 5 mL) were added NaH (19.5 mg, 0.49 mmol) and iodoacetophenone 1a (100 mg, 0.4 mmol). The mixture was stirred at 0°C for 60 min, and then ethyl trifluoroacetate (145 μL, 1.22 mmol) was added dropwise. After stirring at 0°C for 12 h and at room temperature for 12 h, the reaction mixture was acidified with 1N HCl and then neutralized with 1N NaOH. The reaction mixture was extracted with chloroform. The organic layer was washed with brine, dried over Na_2SO_4, filtered and concentrated in vacuo to give brownish oil. The crude product was purified by silica gel column chromatography (AcOEt/hexane/triethylamine= 1:6:0.01) to give 2a as brownish oil in a yield of 35%. ^{1}H NMR ($CDCl_3$) δ, 7.71 (d, J=7.3 Hz, 2H), 7.51 (d, J=7.6 Hz, 2H), 6.30 (s, 1H).

Compound 2a (45.7 mg, 0.134 mmol) and 4-methylsulfonyl-phenylhydrazine hydrochloride (29.8 mg, 0.134 mmol) were dissolved in ethanol (3 ml) and heated under reflux for 4 h. The mixture was allowed to cool before concentration. The crude product was purified by silica gel flash column chromatography (AcOEt/hexane=1:2) to give IMTP 3a as a colorless solid in a yield of 51%. ^{1}H NMR ($CDCl_3$) δ, 7.97 (d, J=8.8 Hz, 2H), 7.74 (d, J=8.5 Hz, 2H), 7.53 (d, J=8.8 Hz, 2H), 6.97 (d, J=8.3 Hz, 2H), 6.79 (s, 1H), 3.08 (s, 3H). FAB-MS calcd for $C_{17}H_{12}IF_3N_2O_2S$ [MH^+]: m/z 493, found 493.

2.2.2. 5-(4-Bromophenyl)-1-[4-(methylsulfonyl)phenyl]-3-trifluoromethyl-1H-pyrazole (BMTP)

BMTP was synthesized in the same manner as IMTP, using bromoacetophenone 1b (100 mg, 0.5 mmol) as a starting material instead of iodoacetophenone 1a (Fig. 1). Compound 2b was obtained in a yield of 31%. ^{1}H NMR ($CDCl_3$) δ, 7.75 (d, J=8.1 Hz, 2H), 7.59 (d, J=7.8 Hz, 2H), 6.43 (s, 1H). Product 2b was then reacted with 4-methylsulfonylphenylhydrazine hydrochloride to give BMTP 3b as a colorless solid in a yield of 78%. ^{1}H NMR ($CDCl_3$) δ, 7.97 (d, J=8.8 Hz, 2H), 7.54 (d, J=8.5 Hz, 2H), 7.53 (d, J=8.8 Hz, 2H), 7.11 (d, J=8.8 Hz, 2H), 6.79 (s, 1H), 3.07 (s, 3H). FAB-MS calcd for $C_{17}H_{12}BrF_3N_2O2S$ [MH^+]: m/z 445, found 445.

2.2.3. 5-(4-Iodophenyl)-1-[4-(aminosulfonyl)phenyl]-3-trifluoromethyl-1H-pyrazole (IATP)

This compound was synthesized by the same method as for IMTP, except that 4-aminosulfonylphenylhydrazine hydrochloride was used instead of 4-methylsulfonylphenylhydrazine hydrochloride (Fig. 1). The product 2a was reacted with 4-aminosulfonylphenylhydrazine hydrochloride to give IATP 3c as a colorless solid in a yield of 85%. ^{1}H NMR ($CDCl_3$) δ, 7.93 (d, J=8.5 Hz, 2H), 7.73 (d, J=8.5 Hz, 2H), 7.47 (d, J=8.5 Hz, 2H), 6.97 (d, J=8.5 Hz, 2H), 6.78 (s, 1H), 4.99 (s, 2H). FAB-MS calcd for $C_{16}H_{11}IF_3N_3O_2S$ [MH^+]: m/z 494, found 494.

2.2.4. 5-(4-Bromophenyl)-1-[4-(aminosulfonyl)phenyl]-3-trifluoromethyl-1H-pyrazole (BATP)

This compound was synthesized using the same method as for BMTP, except that 4-aminosulfonylphenylhydrazine hydrochloride was used instead of 4-methylsulfonylphenylhydrazine hydrochloride. The product 2b was reacted with 4-aminosulfonylphenylhydrazine hydrochloride to give BATP 3d as a colorless solid in a yield of 48%. ^{1}H NMR ($CDCl_3$) δ, 7.94 (d, J=8.5 Hz, 2H), 7.53 (d, J=8.3 Hz, 2H), 7.47 (d, J=8.5 Hz, 2H), 7.11 (d, J=8.3 Hz, 2H), 6.78 (s, 1H), 4.89 (s, 2H). FAB-MS calcd for $C_{16}H_{11}IF_3N_3O_2S$ [MH^+]: m/z 446, found 446.

2.3. Radiolabeling

The radioiodinated IMTP and IATP were obtained by a halogen exchange reaction with sodium ^{125}I-iodine according to the methods of Kiyono et al. [19]. Briefly, BMTP or BATP was added to a mixture of sodium ^{125}I-iodine, ammonium sulfate and copper (II) sulfate pentahydrate in water in a vial. The reaction mixture was heated for 2 h at 140°C. After cooling, the reaction mixture was filtered with a 0.22-μm filter (Ultrafree-MC 0.22-μm filter unit, Millipore, Benford, TX). The filtered solution was applied to a reverse-phase high-performance liquid chromatography (HPLC) column (Cosmosil 5C_{18}-AR-300 Packed Column, 250×10 mm id,

Nacalai Tesque, Kyoto, Japan) and eluted at a flow rate of 2.0 ml/min with 10 mM KH_2PO_4/acetonitrile=1:1 for the purification of ^{125}I-IMTP (R_t=54 min for BMTP, 64 min for IMTP) and 10 mM KH_2PO_4/acetonitrile=53:47 for that of IATP (R_t=58 min for BATP, 70 min for IATP).

The radiochemical purity of the labeled compound was determined by TLC and analytical HPLC. The TLC was performed on a silica gel plate, developed with AcOEt/hexane=1:2 (R_f=0.6 for IMTP and 0.4 for IATP). Analytical HPLC was performed on a 150×4.6-mm id Cosmosil AR-300 column (Nacalai Tesque, Kyoto, Japan) eluted at a flow rate of 1.0 ml/min with 10 mM KH_2PO_4/acetonitrile=1:1 for ^{125}I-IMTP (R_t=18.0 min) and 10 mM KH_2PO_4/acetonitrile=53:47 for ^{125}I-IATP (R_t=17.9 min).

2.4. COX inhibitory potency

Peroxidase inhibitory activities of IMTP and IATP were assessed by measuring the COX-catalyzed oxidation of *N,N,N′,N′*-tetramethyl-*p*-phenylenediamine (TMPD) by hydrogen peroxide using a commercially available kit (Colorimetric COX Inhibitor Screening Assay Kit, Cayman Chemical). Briefly, 10 μl of ovine COX-1 or COX-2 solution was added to a 96-well plate with 150 μl of 0.1 mol/L Tris buffer at pH 8.0, 10 μl of heme solution in DMSO and 10 μl of the test compound (final concentration: 10^{-4}–10^{-9} mol/L). After 5 min of incubation at 25°C, 20 μL of TMPD and 20 μL of 1.1 mM arachidonic acid were added to the mixture. The oxidation of TMPD was monitored by measuring the absorbance of the mixture with a plate reader at 600 nm. SC-58125, meloxicam and indomethacin were used as reference compounds.

2.5. Animal experiments

Animal studies were conducted in accordance with institutional guidelines, and the experimental procedures were approved by the Kyoto University Animal Care Committee.

Biodistribution studies were performed on male Sprague-Dawley rats. ^{125}I-IMTP (74 kBq/rat) or ^{125}I-IATP (74 kBq/rat) was administered to rats under chloral hydrate anesthesia by tail vein injection. At appropriate time points after the administration, the rats were sacrificed by exsanguinations under chloral hydrate anesthesia. Blood and organs were excised and weighed, and the radioactivity was measured with an auto well gamma counter (ARC2000, Aloka, Tokyo, Japan).

Table 1
COX inhibitory potency and selectivity of IMTP, IATP and reference compounds

Compounds	IC_{50} (μM)		IC_{50} ratio (COX-1/COX-2)
	COX-1	COX-2	
IMTP	>100	5.16±2.83	>19
IATP	>100	8.20±1.43	>12
SC58125	>100	1.36±0.44	>73
Meloxicam[a]	>100	29.0	>3.5
Indomethacin[a]	0.08	11.9	0.007

Mean±S.D. of three independent experiments.
[a] Mean of two independent experiments.

Table 2
Biodistribution of ^{125}I-IMTP in rats (%dose/g tissue)

	Time after injection (min)			
	10	30	60	180
Blood	0.08±0.02	0.08±0.01	0.06±0.01	0.04±0.01
Plasma	0.12±0.03	0.12±0.01	0.09±0.01	0.06±0.01
Heart	0.49±0.11	0.50±0.05	0.38±0.06	0.23±0.04
Lung	0.48±0.14	0.42±0.08	0.34±0.04	0.28±0.05
Liver	1.59±0.29	1.53±0.27	1.02±0.15	0.59±0.11
Kidney	0.65±0.14	0.60±0.07	0.42±0.06	0.34±0.05
Pancreas	0.59±0.13	1.26±0.56	0.67±0.11	0.88±0.35
Spleen	0.28±0.06	0.27±0.05	0.23±0.07	0.15±0.04
Stomach	0.27±0.10	0.19±0.04	0.23±0.06	0.17±0.05
Intestine	0.27±0.06	0.38±0.20	0.27±0.04	0.25±0.05
Muscle	0.07±0.02	0.22±0.04	0.17±0.03	0.16±0.01
Thyroid	0.37±0.25	0.54±0.13	0.69±0.30	0.58±0.26
Brain	0.25±0.06	0.23±0.04	0.17±0.03	0.10±0.02
Brain/blood[a]	3.19±0.17	2.87±0.31	2.74±0.24	2.67±0.09

Mean±S.D. for four to five animals.
[a] Brain-to-blood ratio.

2.6. Distribution to blood cells

Distribution of ^{125}I-IATP and ^{125}I-IMTP to blood cells and the effects of several compounds on the distribution were measured by using rat whole blood. Acetazolamide and chlorthalidone were used as reference compounds for binding to carbonic anhydrase (CA), chlorpromazine for binding to the cellular membrane of red blood cells and phenothiazine for binding to hemoglobin. Heparinized whole blood from male Sprague-Dawley rats was preincubated at 37°C with gentle shaking for 5 min and then ^{125}I-IMTP (0.74 kBq) or ^{125}I-IATP (0.74 kBq) was added. After incubation at 37°C for 10 min, chlorpromazine, phenothiazine, acetazolamide or chlorthalidone was added in final concentrations of 10 to 300 μg/ml and then incubated at 37°C for 10 min. A small portion of the blood samples was counted in an auto well gamma counter (Cobra II Auto-

Table 3
Biodistribution of ^{125}I-IATP in rats (%dose/g tissue)

	Time after injection (min)			
	10	30	60	180
Blood	0.63±0.08	0.53±0.03	0.44±0.03	0.45±0.05
Plasma	0.14±0.02	0.12±0.01	0.11±0.01	0.10±0.01
Heart	0.86±0.12	0.62±0.03	0.57±0.03	0.56±0.03
Lung	0.77±0.06	0.58±0.03	0.53±0.05	0.55±0.04
Liver	1.89±0.28	1.31±0.14	1.13±0.12	1.15±0.15
Kidney	0.92±0.11	0.64±0.03	0.55±0.05	0.58±0.06
Pancreas	0.77±0.07	0.79±0.06	0.71±0.06	0.78±0.18
Spleen	0.58±0.07	0.44±0.03	0.39±0.03	0.36±0.02
Stomach	0.24±0.04	0.19±0.06	0.24±0.04	0.22±0.06
Intestine	0.26±0.04	0.29±0.04	0.32±0.07	0.36±0.04
Muscle	0.23±0.06	0.28±0.01	0.27±0.03	0.29±0.03
Thyroid	0.58±0.18	0.47±0.14	0.60±0.07	0.51±0.17
Brain	0.23±0.02	0.22±0.02	0.21±0.01	0.20±0.01
Brain/blood[a]	0.36±0.05	0.42±0.03	0.48±0.03	0.45±0.05

Mean±S.D. for five animals.
[a] Brain-to-blood ratio.

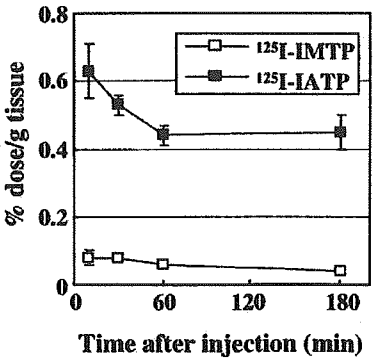

Fig. 2. Levels of ^{125}I-IMTP and ^{125}I-IATP in the blood. Mean±S.D. for four to five animals.

Gamma, Packard, Tokyo, Japan), and the rest were centrifuged for 1 min and the plasma separated. A small portion of the plasma samples was also counted. Hematocrit was measured using an i-STAT portable clinical analyzer (i-STAT, East Windsor, NJ). Distribution of the labeled compounds to blood cells was calculated as follows:

$$T = [1 - C_P/C_B \times (100 - H_t)/100] \times 100$$

where T is the distribution% to blood cells, C_P and C_B are the radioactivity in blood and plasma, respectively, and H_t is the hematocrit value.

2.7. Statistical analysis

Data are presented as mean values with the standard deviation, unless otherwise noted. Statistical analysis was performed by one-way ANOVA followed by Bonferroni–Dunn test for post hoc comparisons. Statistical significance was defined as a two-tailed P value <.05/6 (i.e., .0083).

3. Results

3.1. Synthesis and radiolabeling

IMTP, BMTP, IATP and BMTP were obtained with overall yields of 18%, 25%, 26% and 17%, respectively, from the starting material 1a or 1b. The radiosynthesis of ^{125}I-IMTP and ^{125}I-IATP was achieved with an iodine–bromide exchange reaction. ^{125}I-IMTP and ^{125}I-IATP were obtained with no carrier being added by the following separation from the precursors (BMTP and BATP) using reverse-phase HPLC. The radiochemical yields were 42% for ^{125}I-IMTP and 35% for ^{125}I-IATP, and the radiochemical purities were >95% for both of the labeled compounds.

3.2. COX inhibitory potency

IMTP and IATP inhibited COX-2 in a concentration-dependent manner, while they showed no inhibitory potency for COX-1 even at the highest concentration examined. Table 1 summarizes the IC_{50} values of the test compounds. The IC_{50} values of IMTP and IATP were 5.16 and 8.20 μM for COX-2 and >100 μM for COX-1. The COX-2 inhibitory potency of IMTP and IATP was higher than that of meloxicam (IC_{50}=29.0 μM) and comparable to that of SC-58125 (IC_{50}=1.36 μM). The IC_{50} ratio (COX-1/COX-2) for IMTP, IATP, SC-58125 and meloxicam was >19, 12, 73 and 3.5, indicating a high isoform selectivity of IMTP and IATP for COX-2.

3.3. Biodistribution

The biodistribution of ^{125}I-IMTP and ^{125}I-IATP is shown in Tables 2 and 3, respectively. The level of radioactivity for ^{125}I-IMTP in the blood decreased more rapidly than that for ^{125}I-IATP (Fig. 2). The radioactivity in the blood was 0.04 %dose/g tissue for ^{125}I-IMTP and 0.45 %dose/g tissue for ^{125}I-IMTP at 180 min after the tracer administration. At 10 min after the injection, high levels of the radioactivity were found in the liver and kidneys for both compounds. ^{125}I-IATP showed relatively higher levels of radioactivity in the heart and lung. Both compounds showed no marked accumulation in the stomach and thyroid. Significant levels of radioactivity were found in the brains of rats, with brain-to-blood ratios of 2.67–3.19 for ^{125}I-IMTP and 0.36–0.48 for ^{125}I-IATP.

3.4. Distribution to blood cells

Distribution of ^{125}I-IATP to blood cells (88.0%) was markedly higher than that of ^{125}I-IMTP (18.1%) as shown

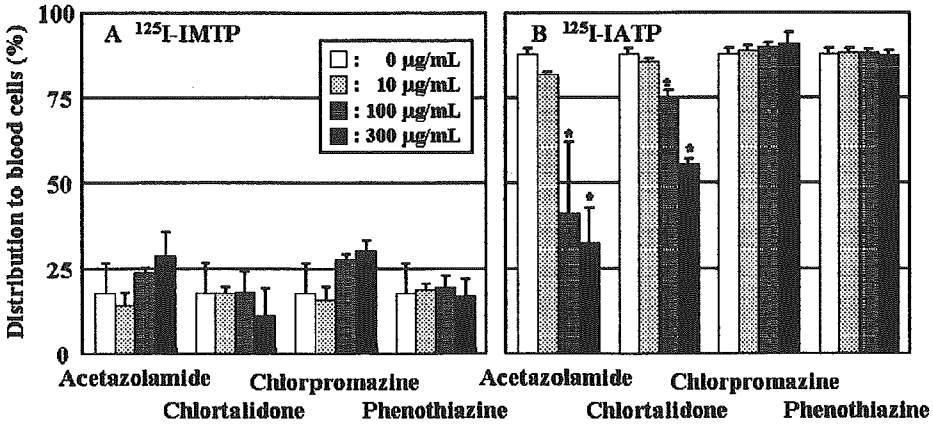

Fig. 3. Distribution of ^{125}I-IMTP (A) and ^{125}I-IATP (B) to blood cells. Mean±S.D. of three measurements. *P<.05/6 (i.e., .0083).

in Fig. 3. The distribution of ^{125}I-IATP to blood cells was significantly decreased by CA inhibitors (acetazolamide and chlorthalidone), but not by chlorpromazine or phenothiazine. The distribution of ^{125}I-IMTP to blood cells was not affected by any of the compounds used in the present study.

4. Discussion

In the present study, we synthesized a methyl sulfone-type COX-2 inhibitor, 5-(4-iodophenyl)-1-[4-(methylsulfonyl)phenyl]-3-trifluoromethyl-1*H*-pyrazole (IMTP). The potential of radioiodinated IMTP for imaging COX-2 expression was evaluated in comparison with a ^{125}I-labeled celecoxib analogue with a sulfonamide moiety (^{125}I-IATP). The major findings in the present study can be summarized as follows: (1) IMTP had a high inhibitory potency and selectivity for COX-2. (2) ^{125}I-IMTP showed a biodistribution compatible with the known distribution of COX-2. (3) The blood clearance of ^{125}I-IMTP was much faster than that of ^{125}I-IATP. (4) ^{125}I-IATP showed markedly higher distribution to blood cells than ^{125}I-IMTP, which was decreased by CA inhibitors. These results demonstrate that the substitution of the sulfonamide moiety to a methyl sulfone moiety effectively improved the blood clearance of the compound, indicating the loss of the cross reactivity with CA in ^{125}I-IMTP. Methyl sulfone-type COX-2 inhibitors may be a preferential candidate as radiopharmaceuticals for COX-2 expression.

The methyl sulfone moiety and sulfonamide moiety at position 4 of the 1-phenyl ring are considered to be optimal for COX-2 selectivity [11]. In this regard, several COX-2 inhibitors with a methyl sulfone or sulfonamide moiety were recently radiolabeled and preliminarily evaluated as imaging agents [12–14,16]. However, the effects of these moieties on the pharmacokinetics of the labeled tracers have not been determined. Our results clearly showed that the substitution of the sulfonamide moiety to the methyl sulfone moiety effectively improved the blood clearance of the compound (Fig. 2). In addition, the high distribution of ^{125}I-IATP to blood cells was significantly inhibited by CA inhibitors (Fig. 3). Recently, it was reported that sulfonamide-type celecoxib analogues show high affinity to carbonic anhydrase (CA) [18]. Agents containing sulfonamides (e.g., acetazolamide) have been widely used in clinical medicine to inhibit carbonic anhydrase (CA) [17,18]. The slow blood clearance of ^{125}I-IATP can be ascribed to the affinity of its sulfonamide moiety to CA in erythrocytes [17,18]. These results indicate the feasibility of methyl sulfone-type COX-2 inhibitors as radiopharmaceuticals for COX-2 expression.

Although COX-2 is an inducible isoform, it is predominantly found in the normal brain and kidneys [20]. The preferential uptakes of ^{125}I-IMTP and ^{125}I-IATP in these organs were compatible with the expression of COX-2 in these organs. The high brain-to-blood ratio of ^{125}I-IMTP indicates the feasibility of this compound for COX-2 imaging in the brain. On the other hand, no marked ^{125}I-IMTP accumulation was observed in the stomach or thyroid, indicating its stability to in vivo deiodination. The present results using ^{125}I-IMTP are consistent with those using ^{18}F-SC-58125, which showed preferential uptakes in the brain and kidneys with rapid blood clearance [12]. SC-58125 is a methyl sulfone-type COX-2 inhibitor that has the same structure as IMTP except that the fluorine in SC-58125 is replaced with iodine in IMTP. These results further confirm the potentials of methyl sulfone-type COX-2 inhibitors as radiopharmaceuticals for COX-2 expression.

In the present study, we determined the biodistribution of the labeled compounds at several time points within 3 h, considering that small animals generally show rapid pharmacokinetics compared with that in humans. Consequently, we demonstrated that ^{125}I-IMTP showed preferential uptakes in the brain and kidneys with much faster blood clearance than ^{125}I-IATP. Time points <3 h appear to be appropriate to extrapolate the pharmacokinetics in humans from those in rats. We generally perform experiments to block the uptake of a candidate compound in tissues by coinjecting the nonradioactive compound, in order to confirm its specific distribution. In the present study, however, we did not perform such blocking experiments, because the physiological expression levels of COX-2 are relatively low compared with those in the pathological state. Such blocking experiments do not appear to be suitable to demonstrate the specific distribution of radiolabeled COX-2 inhibitors. McCarthy et al. [12] failed to obtain in vivo blocking data to show the specific binding of a radiotracer (^{18}F-SC58125) to COX-2 in rats. Contrarily, de Vries et al. [13] indicated the specific binding of ^{18}F-desbromo-DuP-697 by blocking experiments in rats. Experiments in animal models with higher COX-2 expression may be necessary to assess the specific binding of tracers to COX-2. We must await further studies to achieve this goal. Experiments to demonstrate the advantage of longer half-lives of SPECT nuclides are also required.

The COX-2 inhibitory potency of IMTP and IATP was higher than that of meloxicam and was comparable to that of SC-58125, suggesting that the introduction of iodine at position 4 of the 5-phenyl ring did not largely affect the COX-2 inhibitory potency. In addition, IC_{50} ratios (COX-1/COX-2) for IMTP and IATP showed high isoform selectivity of these compounds for COX-2 (Table 1), indicating that the selectivity of IMTP and IATP for COX-2 is comparable to celecoxib [21,22]. These results were consistent with the consideration on the structure–activity relationship reported by Herschman et al. [11] and suggest that the introduction of iodine at position 4 of the 5-phenyl ring is acceptable.

5. Conclusion

A radioiodinated COX-2 inhibitor, ^{125}I-IMTP, was synthesized. Our results showed a high inhibitory potency